Evolution of atmospheric particulate pollutions for the Hauts-de-France region and their impact on the solar environment : Past, present and future scenarios

G. Chesnoiu[1], N. Ferlay[1], P. Nabat[2], M. Mallet[2], F. Auriol[1], M. Catalfamo[1], I. Jankowiak[1], I. Chiapello[1]

1 - Université de Lille, CNRS, UMR 8518 - LOA, Lille F-59000, France
2 - UMR 3589 - CNRM, CNRS, Toulouse F-31057, France

Contact : gabriel.chesnoiu@univ-lille.fr

Introduction

Global mean energy budget of the Earth (IPCC, 2021)

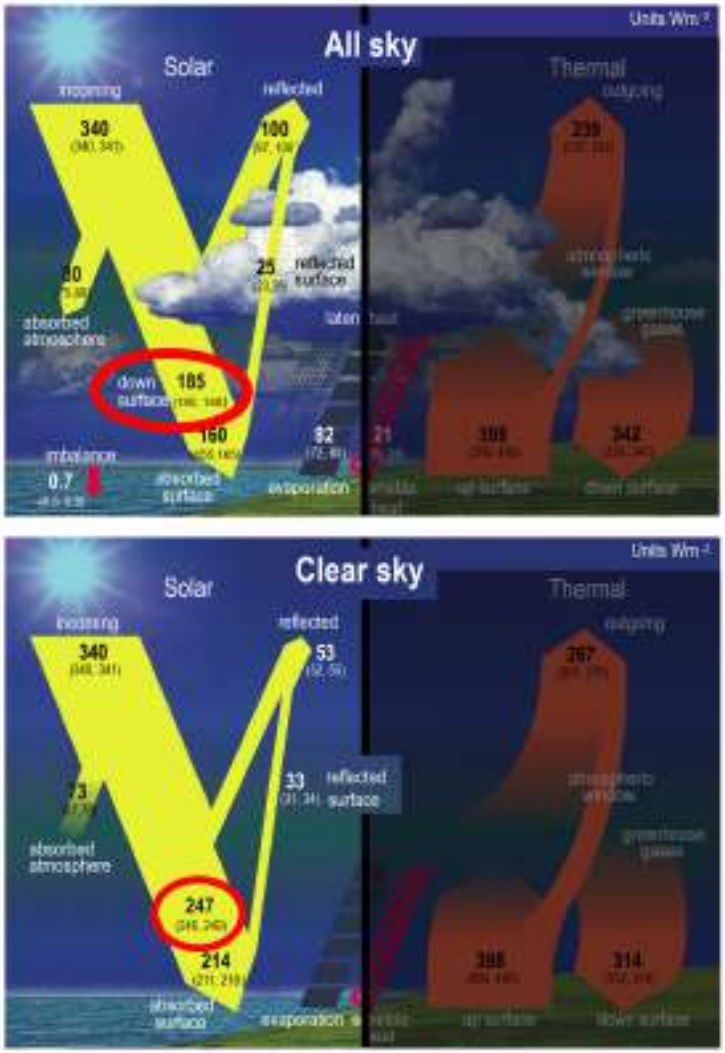

- Aerosols & clouds greatly affect the Earth's energy balance and PV production by absorption and scattering of the incoming solar radiation
- High spatial/temporal variability of their occurrences & properties

  $\rightarrow$ Difficult to distinguish and quantify the respective impacts of clouds & aerosols
- Need of regional studies of both radiation & atmospheric parameters

Objective: Analyze the present and future variability of the surface solar irradiance & PV potential in the North of France

1 Introduction

2 Methodology
- ATOLL measurements in Lille
- Classification of the sky conditions in Lille
- Configuration of ALADIN-climat simulations over the extended Hauts-de-France (HdF) region

3 Results
- Observed climatology of the irradiance and atmospheric content in Lille
- Validation of ALADIN-climat HINDCAST simulations
- Analysis of the future variability

4 Supplements

Presentation of the ATOLL (ATmospheric Observations in LiLle) measurement platform (50.61167°N, 3.14167°E)

Solar resource

Kipp & Zonen fluxmeters (since 2009) – 1-min resolution

Pyrheliometer (CH1)
Direct normal irradiance, **DNI**
⇓
Beam horizontal irradiance
BHI = $cos(SZA) \times DNI$

Pyranometer (CMP22)
Diffuse irradiance, **DHI**

⇒ **Global** irradiance, **GHI = BHI + DHI**

Atmospheric composition

AERONET sunphotometer CIMEL CE-318 (since 1994)

- Aerosol Optical Depth (AOD) & Angström Exponent (AE) in clear-sun conditions
- Size distribution & refractive index inversions [Dubovik and King, 2000]
- Integrated Precipitable Water Content (PWC) derived from measurements at 940nm

Additional observations

- Sky images from a CMS Schreder VIS-J1006 since 2009 (3-min resolution)
- Meteorological observations of relative humidity, temperature, wind speed & direction (since 2005)

⇒ Coincident data of atmospheric content & solar resource available over 2010 - 2022

Classification of the sky conditions over Lille

Irradiance based sky condition detection algorithms

- Batlles et al. (2000) → Clear-sun moments
- Garcia et al. (2014) → Clear-sky moments

$\Rightarrow$ *Clear-sun with clouds* $\in (\textit{Batlles} \cap \overline{\textit{Garcia}})$

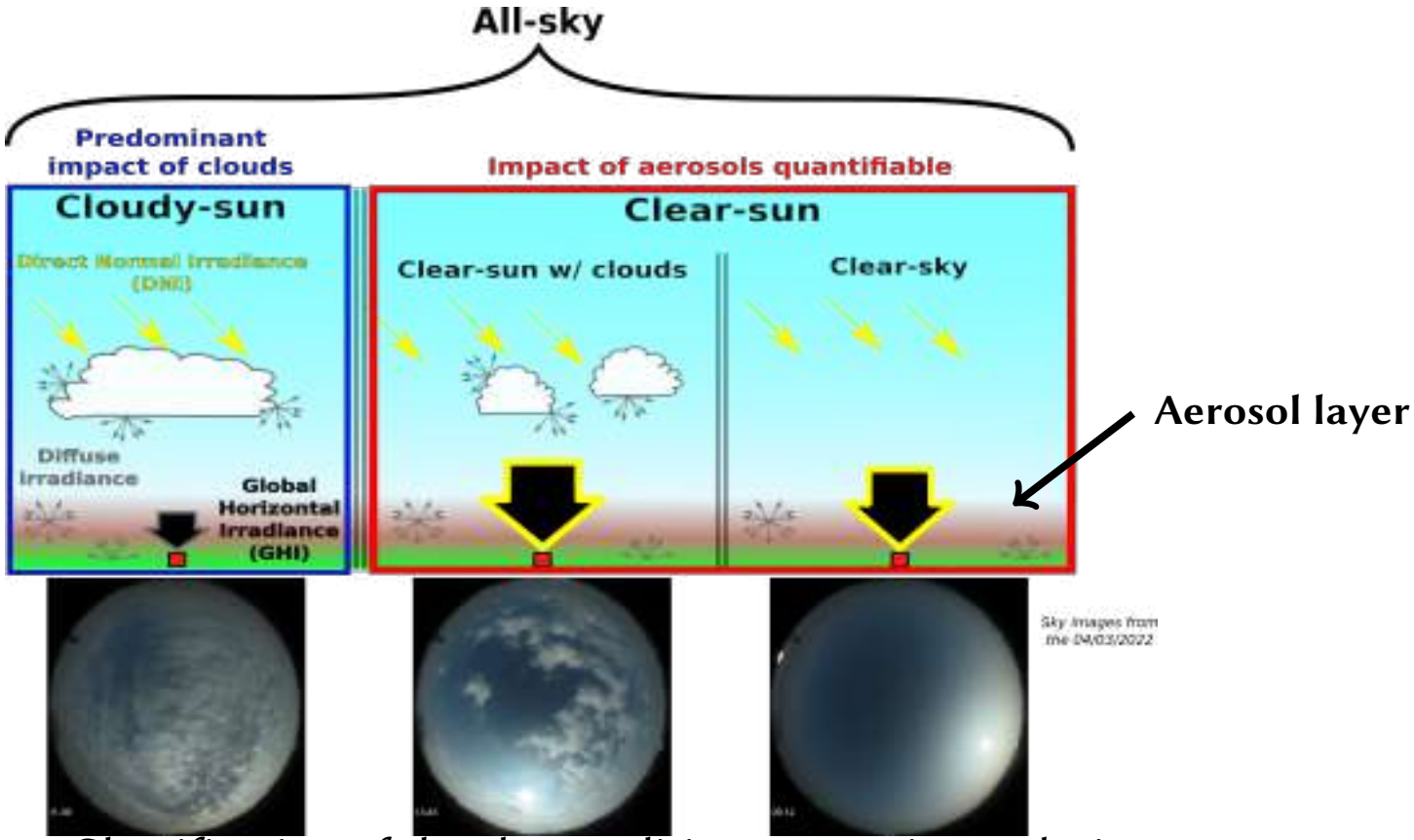

$\Rightarrow$ Classification of the sky conditions at 1-min resolution between [sunrise + 30 minutes; sunset - 30 minutes]

Definition of ALADIN-climat regional climate simulations over HdF

Objective: Study the spatial variability of atmospheric content & irradiances at a regional scale under future climate scenarios

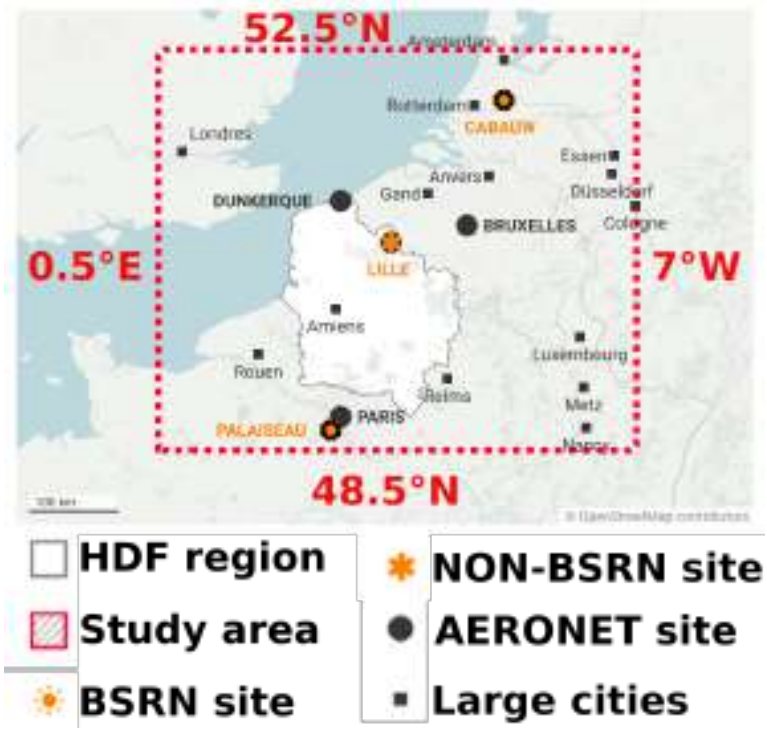

- **Spatial & temporal resolutions : 12x12km & 1h**
  Nabat et al. (2020)
- **Concentrations & properties** (AOD, AE, SSA, g) of **7 aerosol types** (SS, DU, BC, OM, SO_4, NO_3, NH_4)
- Gaseous content (water vapor, ozone, ...)
- **Cloud fraction** (clt) $\rightarrow$ clear-sky criterion of 3.5%
- **Surface solar irradiances** (GHI, BHI, DHI) in **clear-sky and all-sky conditions**
- **Two possible driving models :**
  - ERA5 reanalysis $\rightarrow$ **HINDCAST** (2000 - 2020)
  - GCM CNRM-ESM2-1 $\rightarrow$ **HIST** (2005-2014) and **SSPs 1-1.9 & 3-7.0** (2045-2054, 2091-2100)

Initial configuration showed **large overestimation of the AOD in spring due to NO_3 aerosols $\rightarrow$ all monthly NH_3 emissions cut by 25%** in present configuration

1 Introduction

2 Methodology
- ATOLL measurements in Lille
- Classification of the sky conditions in Lille
- Configuration of ALADIN-climat simulations over the extended Hauts-de-France (HdF) region

3 Results
- Observed climatology of the irradiance and atmospheric content in Lille
- Validation of ALADIN-climat HINDCAST simulations
- Analysis of the future variability

4 Supplements

Seasonal climatology of the sky conditions, aerosol optical properties and solar resource measured in Lille over 2010 - 2022

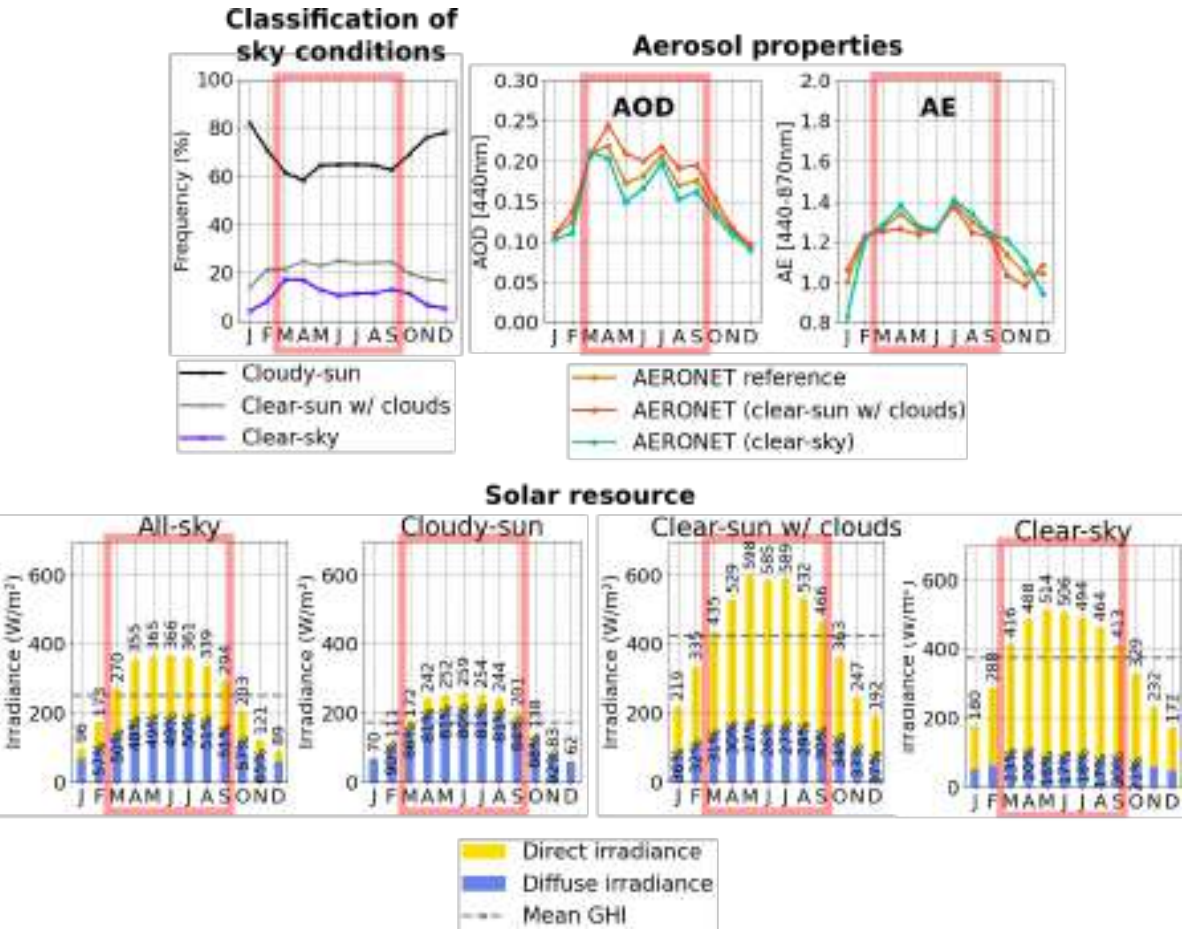

- **High & variable influence of clouds with on average :**
  - ↪ Clear-sky ∼ 11%
  - ↪ Clear-sun w/ clouds ∼ 22%
  - ↪ Cloudy-sun moments ∼ 67%
- **Relatively polluted site:**
  - ↪ 70% of AOD values > 0.1
  - ↪ Mostly fine aerosols ($\overline{AE} > 1$)
- Spring & summer characterized by :
  - ↪ **Min influence of clouds (clear-sky ∼ 10-20%)**
  - ↪ **Max influence of aerosols (AOD_{440nm} > 0.15)**
  - ↪ **Max of solar resource due to SZA and day length**

Observed trends in sky conditions frequency, AOD and surface irradiance in Lille over 2010-2022

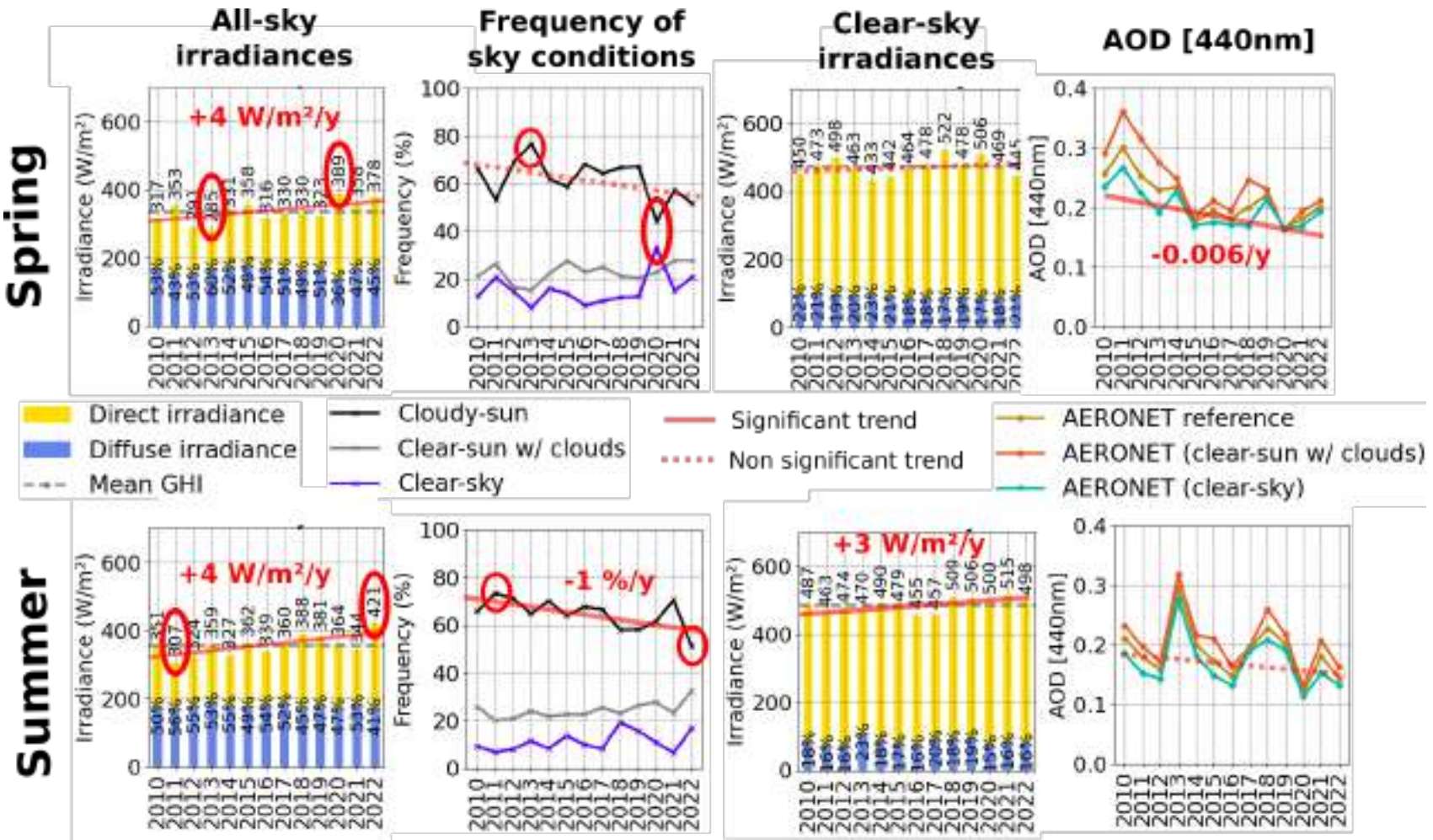

Validation of ALADIN-climat hourly HINDCAST simulations over 2010 - 2020 (1/2)

Monthly variability over the extended HdF region (2010 - 2020)
6 AERONET sites (France, Belgium, Netherlands)

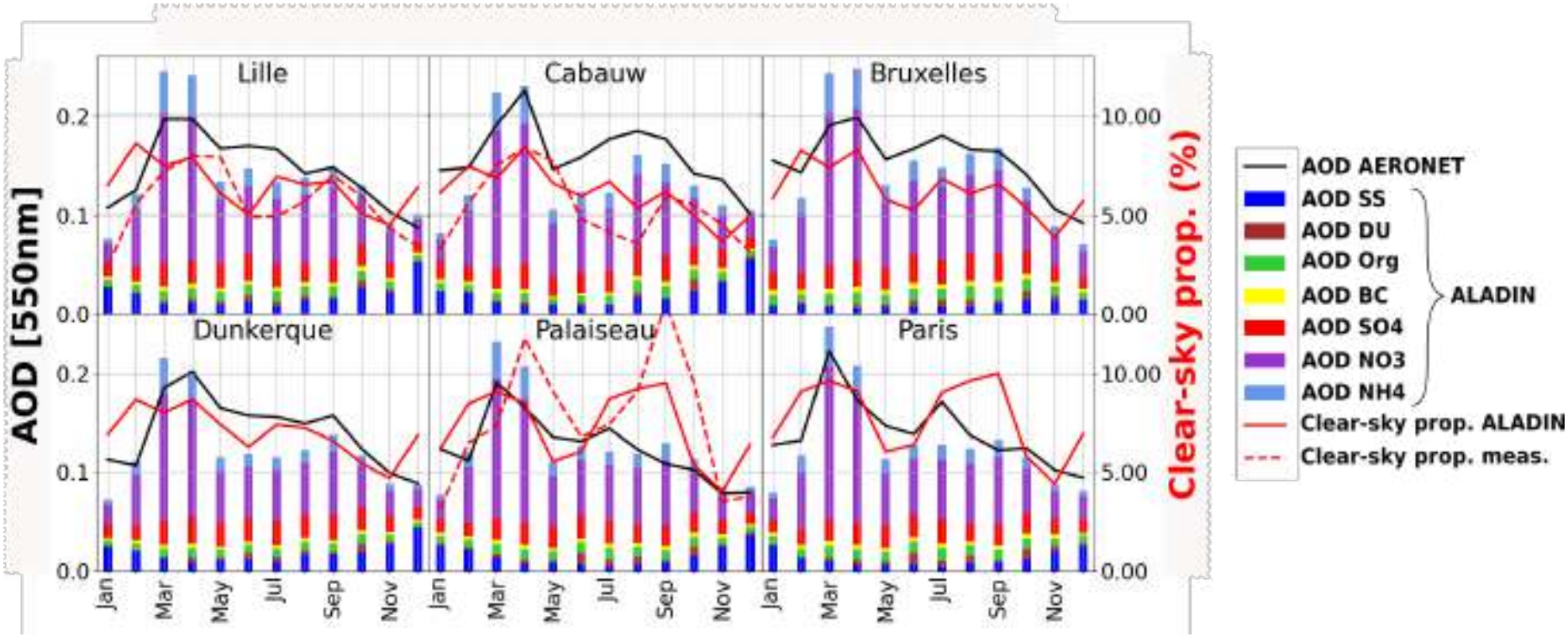

Good representation of the seasonal variability of both AOD and clear-sky frequency

Validation of ALADIN-climat hourly HINDCAST simulations over 2010 - 2020 (2/2)

Comparisons to measurements of 6 AERONET sites in clear-sun conditions

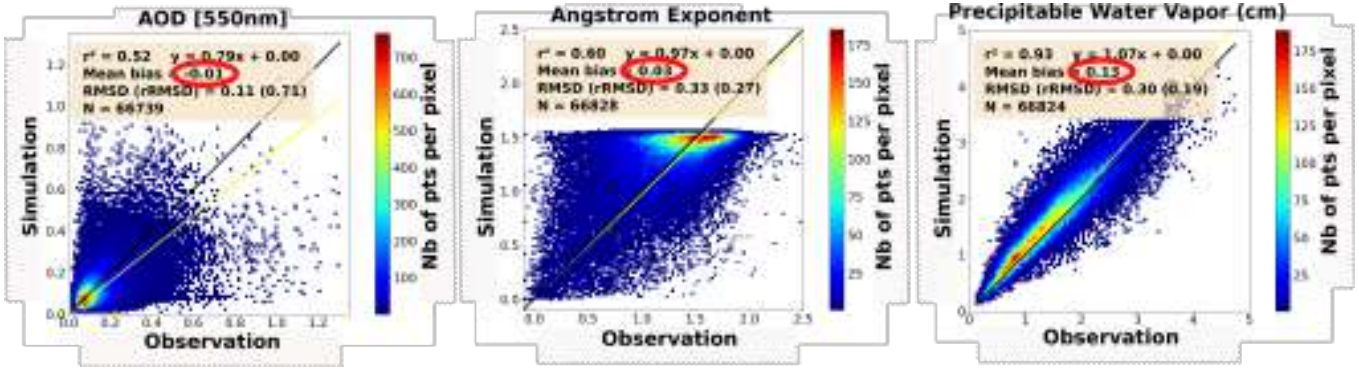

Comparisons to irradiance measurements of 3 sites in clear-sky conditions

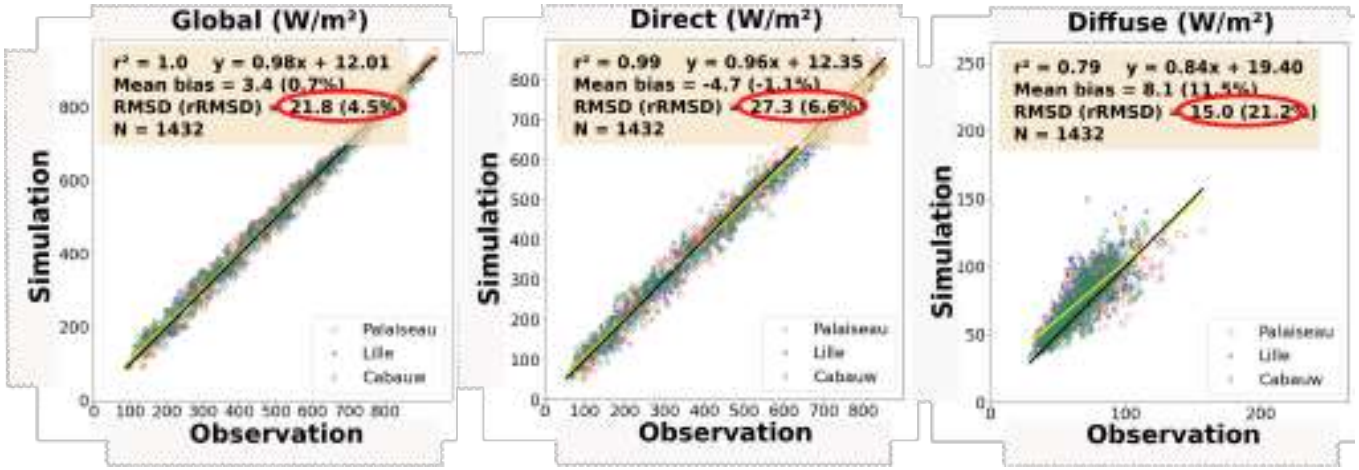

⇒ Overall satisfactory simulations of atmospheric content & irradiances

Aerosol direct radiative effects (DRE) in clear-sky conditions

$$DRE = GHI_{clear\text{-}sky} - GHI_{pristine}$$

- $GHI_{clear\text{-}sky}$: Global irradiance (GHI) under clear-sky conditions
- $GHI_{pristine}$: Simulated clear-sky GHI under pristine-like conditions (AOD = 0)

Mean observed DRE in Lille in clear-sky conditions over 2010-2022 (W/m²) [%]

Winter	Spring	Summer	Autumn	Year
(-15.6) [-6.4]	(-21.4) [-5.9]	(-18.8) [-4.8]	(-19.2) [-5.5]	(-19.7) [-5.5]

Mean simulated clear-sky DRE over the extended HdF region (2010-2020)

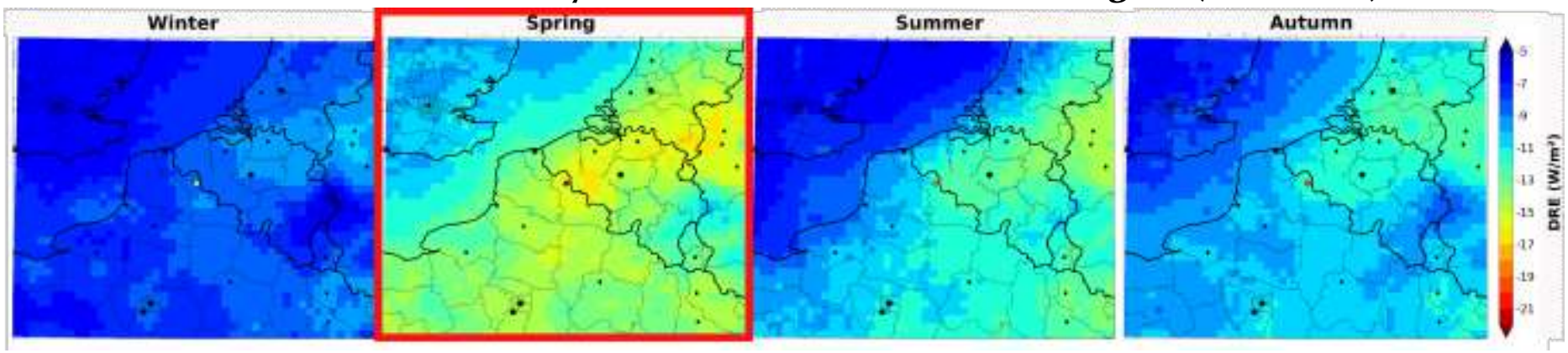

ALADIN-climat HINDCAST

- **Min/Max DRE observed in Winter/Spring in Lille well simulated by ALADIN although underestimated by ∼ 5-6 W/m² for all seasons**
- **Strongest effects in the Benelux region**

Comparisons between HINDCAST and HIST simulations over 2005-2014 in clear-sky conditions in spring

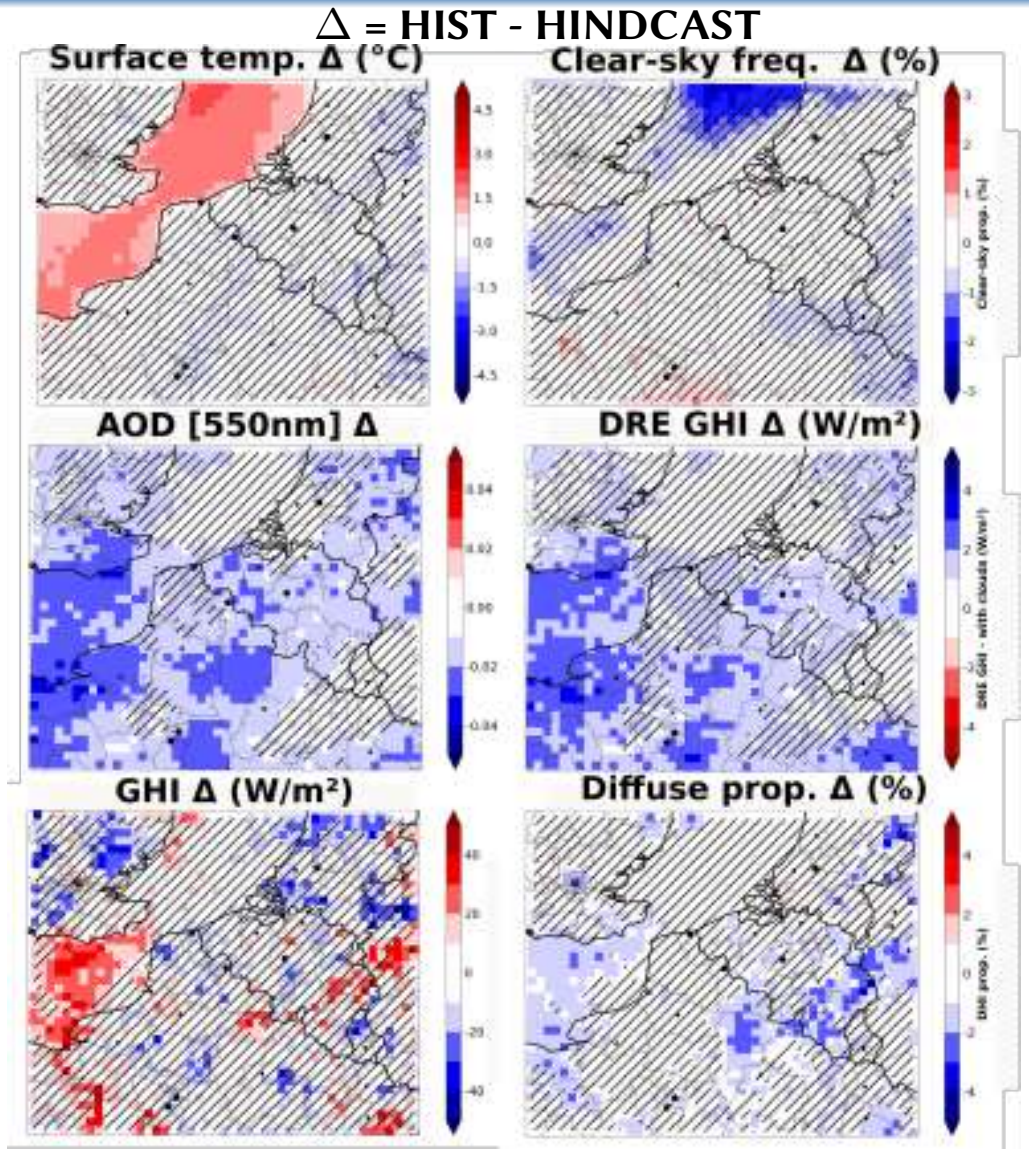

- Good agreement for the T° although sea temp. is overestimated $\sim$ 1-1.5°C
- Good agreement for the clear-sky frequency except at North of the English channel ($\Delta \sim -2\%$)
- AOD & DRE underestimated in HIST simulations by $\sim$ 0.01-0.02 (1-2 W/m²)
- Good agreement for the irradiances

Analysis of the future variability in spring of the atmospheric content & irradiances for ALADIN-climat regional simulations under two contrasting scenarios :

- ↪ **SSP1-1.9** – Optimistic :
  - ↪ Fast decrease in AOD & GHG
  - ↪ Stable radiative forcing & surface temperatures
- ↪ **SSP3-7.0** – Pessimistic :
  - ↪ Large increase in GHG but stable AOD
  - ↪ Large increase in radiative forcing & surface temp.

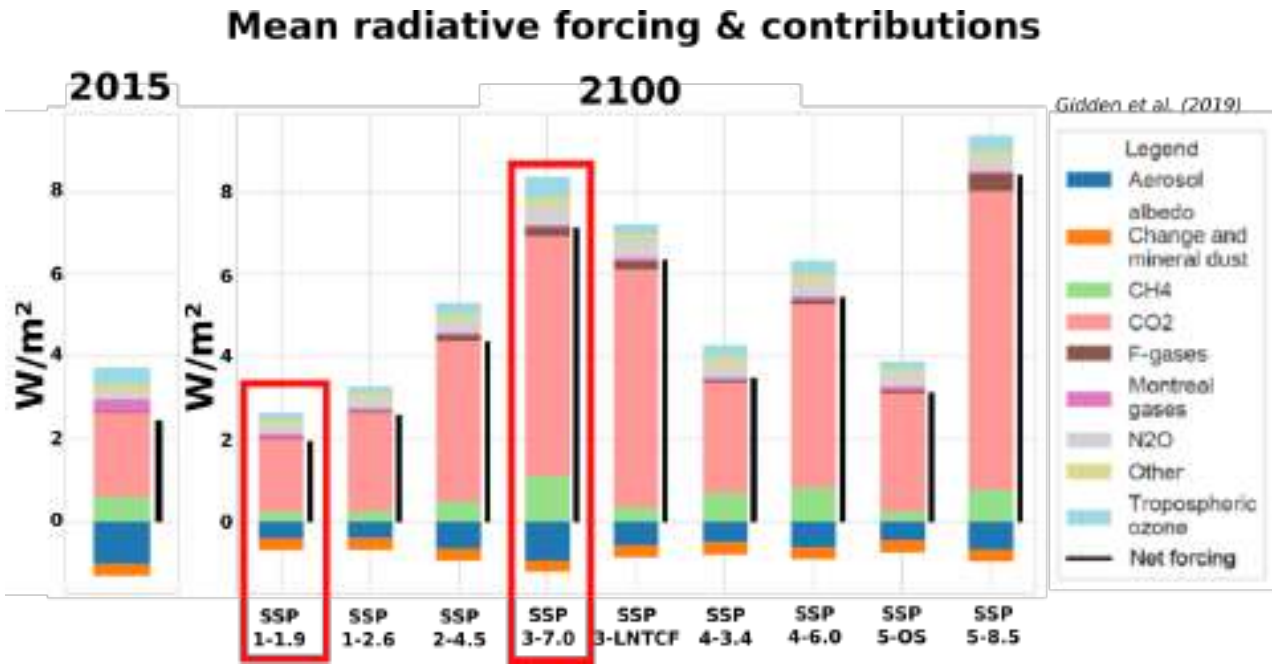

Future regional evolution of the clear-sky frequency in spring

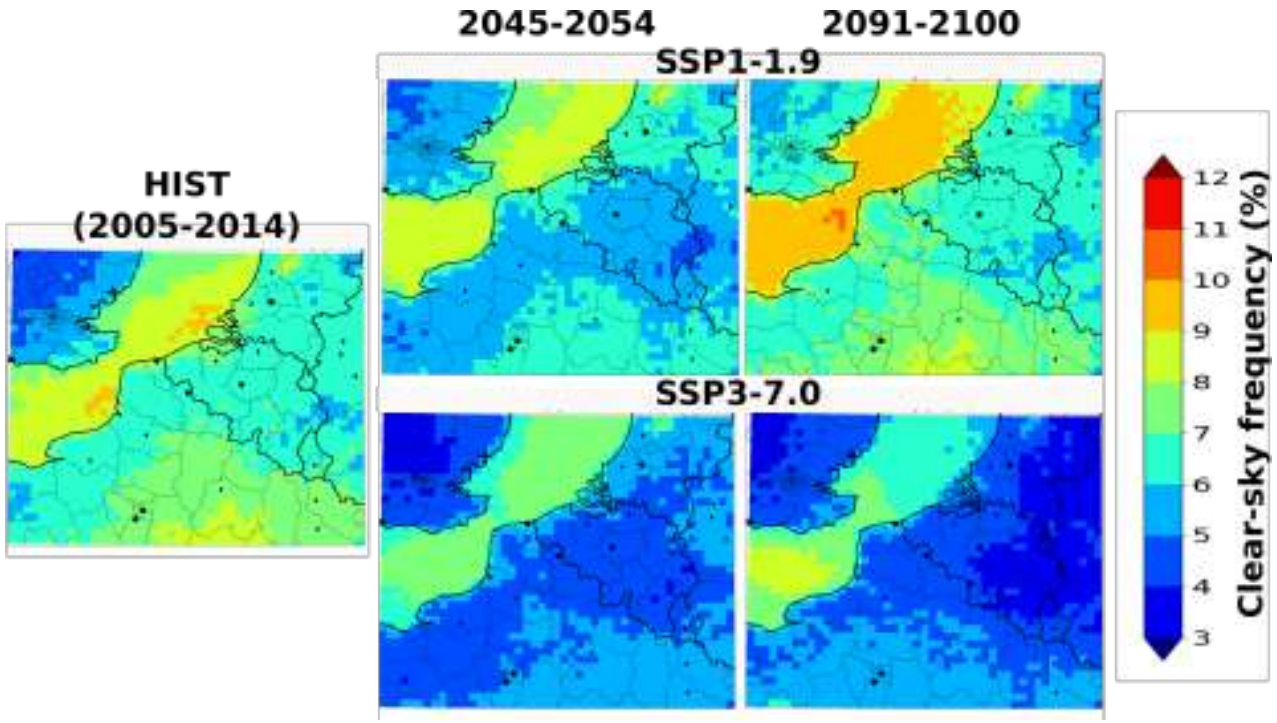

- **Strong spatial variability with values ranging from $\sim$ 4% to 8-9%**
- No significant evolution under SSP1-1.9
- **Decrease under SSP3-7.0 :**
  - **Loss of around -1 to -2% over the sea**
  - **Greater loss over land $\sim$ -2 to -3%**

Future regional evolution of the AOD & its clear-sky DRE in spring

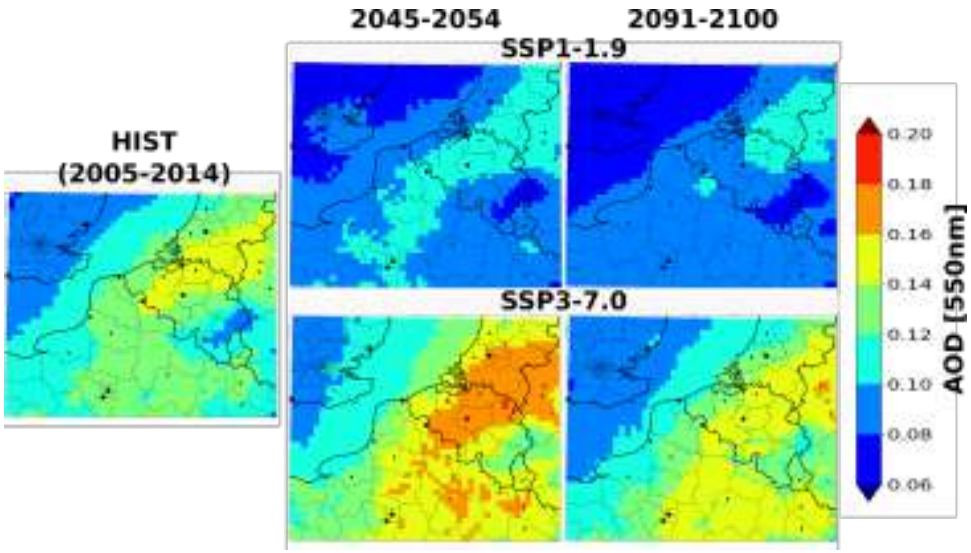

- SSP1-1.9 :
  - **Quick decrease ∼ -0.02 to -0.06**
  - **Spatial homogenization ?**
- Increased AOD under SSP3-7.0 which is stronger by mid century ∼ +0.02

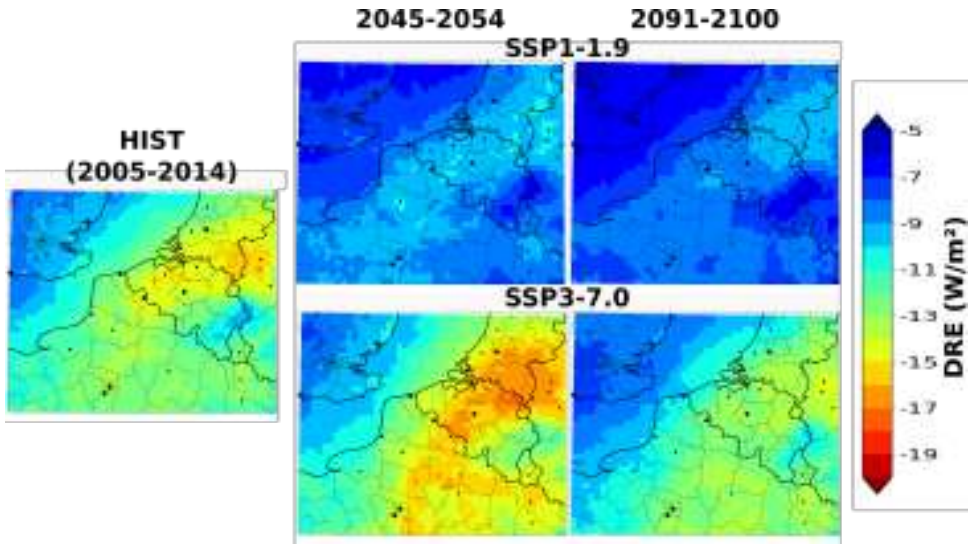

- Similar behaviour for the DRE although there is a small decrease around North-West corner under SSP3-7.0

Future regional evolution of the clear-sky irradiance in spring

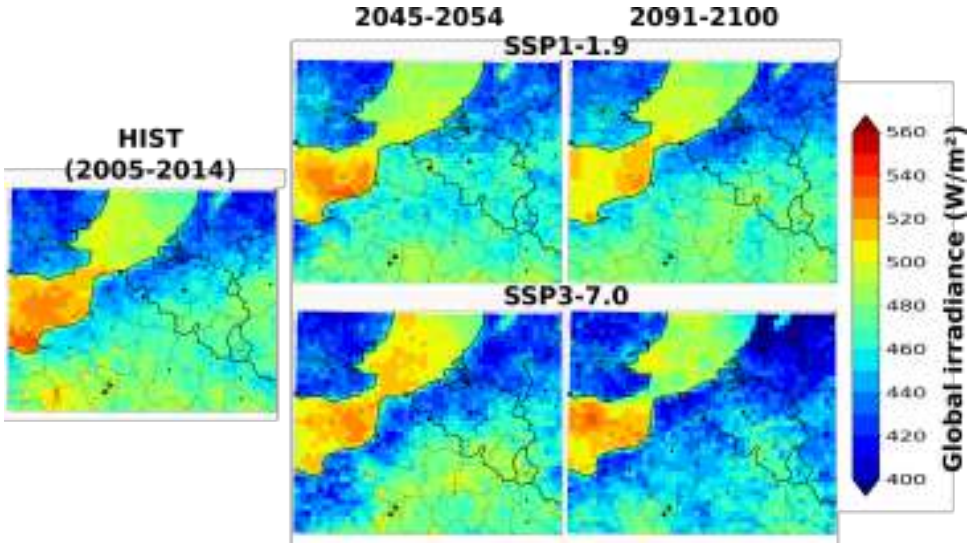

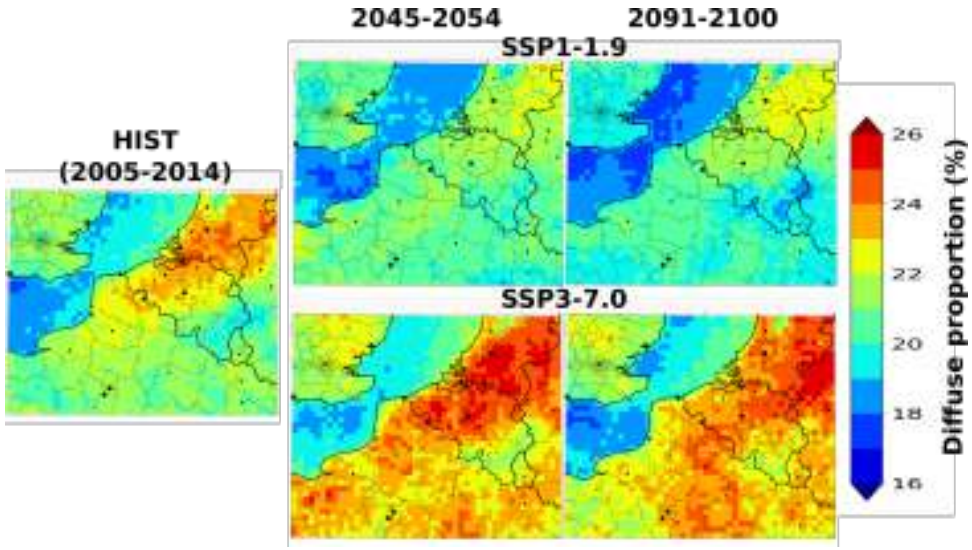

- **Strong spatial differences**
- No significant evolution under SSP1-1.9
- **Decrease in GHI under SSP3-7.0 $\sim$ 50 W/m² over the South-West & Benelux regions**

- **Decrease in DHI prop under SSP1-1.9 from $\sim$ 20-25% to 16-23%**
- **Increase under SSP3-7.0 of around 1-3%**

Conclusions

- **Analysis of the contributions of clouds & aerosols to surface solar irradiance variability in North of France over 2010-2022 based on :**
  - ↪ Coincident irradiance & photometric ground measurements from ATOLL
  - ↪ A classification of the sky conditions at 1-min resolution
  - ↪ RCM ALADIN-climat simulations & additional AERONET/BSRN ground measurements
- **Important and highly variable influence of both clouds & aerosols with maximum effects in spring and summer**
- **Satisfactory regional simulations of atmos. content & irradiances**
- **Provisional regional analysis of the future variability in clear-sky conditions in spring for SSPs 1-1.9 & 3-7.0:**
  - ↪ Decrease in clear-sky freq. under SSP3-7.0 $\sim$ 2-3%
  - ↪ Important decrease in AOD & DRE under SSP1-1.9
  - ↪ Stable AOD & DRE under SSP3-7.0 with increase up to 2050 then decrease
  - ↪ Stable global irradiance for both scenarios with decreased (increased) diffuse irradiance under SSP 1-1.9 (SSP3-7.0)

Perspectives

- **Further analysis of the future variability of atmospheric content and surface solar radiation :**
  - ↪ Investigation of the other parameters (SZA, SSA, g, etc.)
  - ↪ Analysis of the all-sky irradiances
  - ↪ Study of the variability for other seasons
  - ↪ Assessment of the contribution of the different aerosol types
- **Complementary analysis of the PV production over the extended HdF region and its variability**

Thank you for your attention

Supplements

Validation of the cloud-screening methods

Method: Comparisons against ground observations based on sky images from the VIS-J1006 for the months of January and May 2018 (3-min resolution)

Confusion matrix							
		TP	TN	FN	FP	Precision	Risk
	Definition	Filter → Clear Obs → Clear	Filter → Cloudy Obs → Cloudy	Filter → Cloudy Obs → Clear	Filter → Clear Obs → Cloudy	$\frac{TP}{TP+FP}$	$\frac{FP+FN}{FP+FN+TP+TN}$
Clear-sky (Garcia)	Nb of cases (% of cases)	1549 (12.5%)	10186 (82.1%)	328 (2.6%)	340 (2.7%)	82%	5%
Clear-sun (Batlles)		2702 (21.8%)	8247 (66.5%)	98 (0.8%)	1356 (10.9%)	67%	12%

Representativity of the aerosol variability for coincident clear-sun/sky measurements

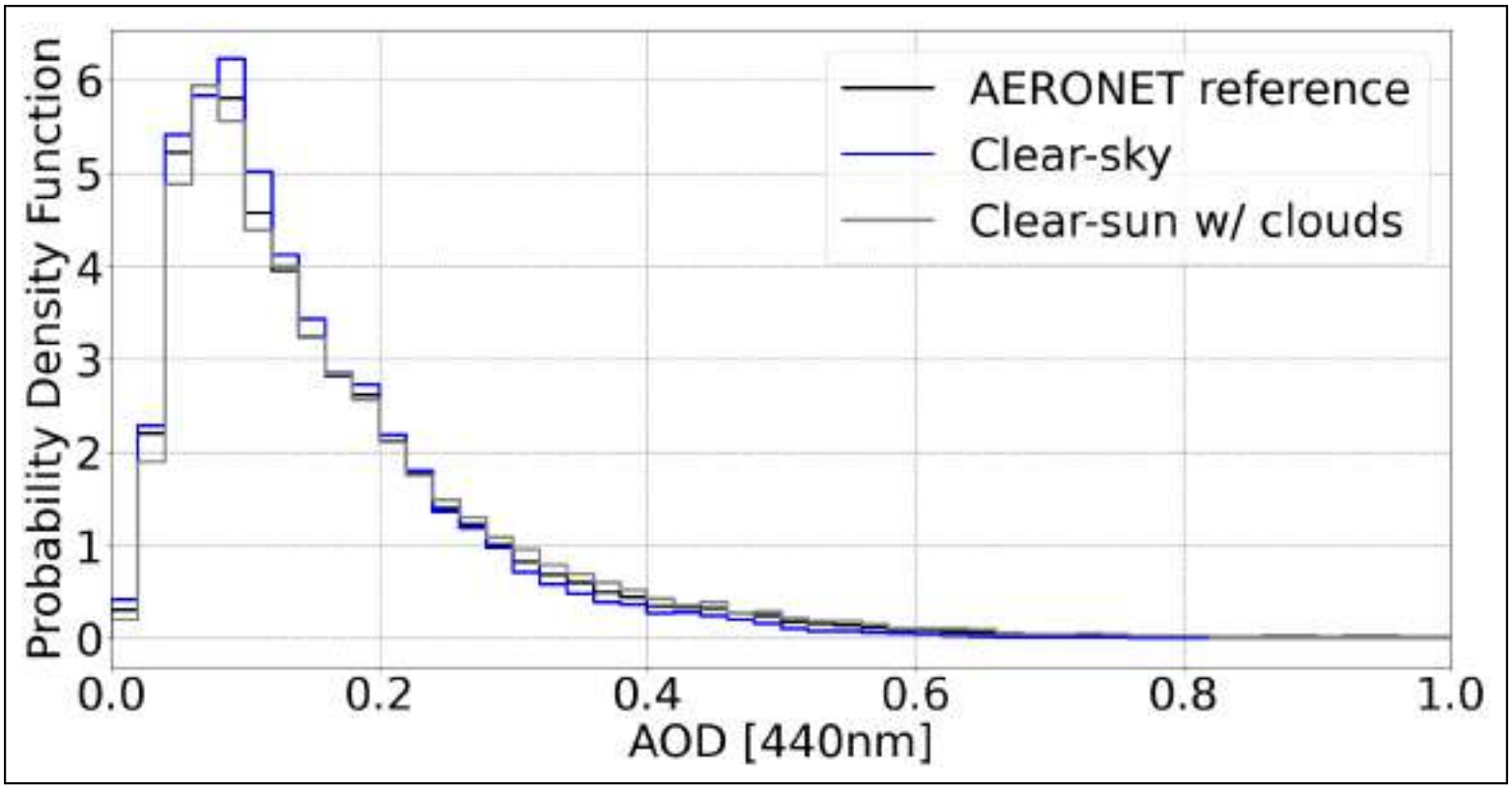

PDF of AOD [440nm] when considering all AERONET measurements (black line) as well as only observations coincident with clear-sky (blue line) and clear-sun with clouds (grey line) irradiance measurements.

Monthly variability of all the parameters

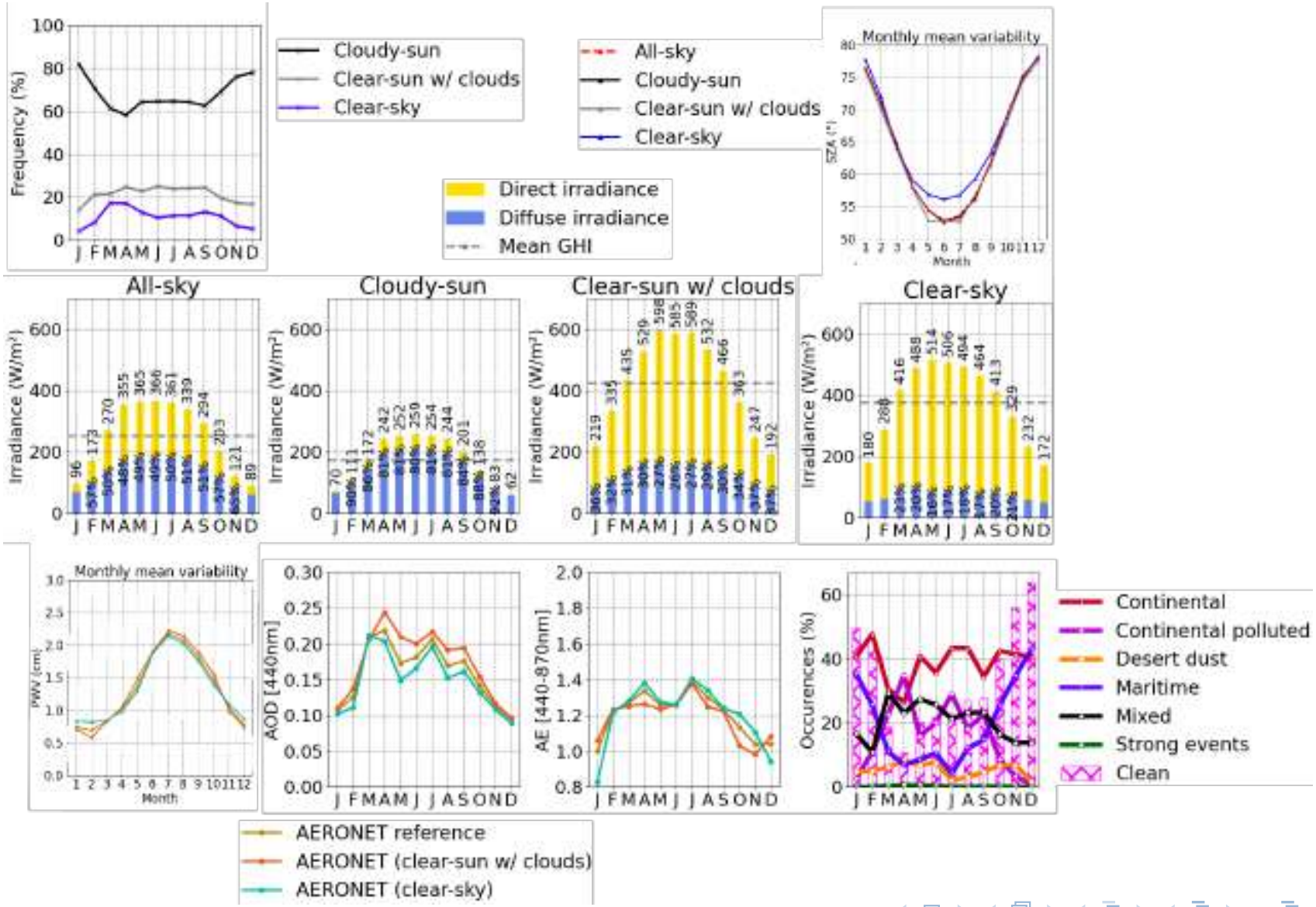

Yearly variability of all the parameters in Spring over 2010-2022

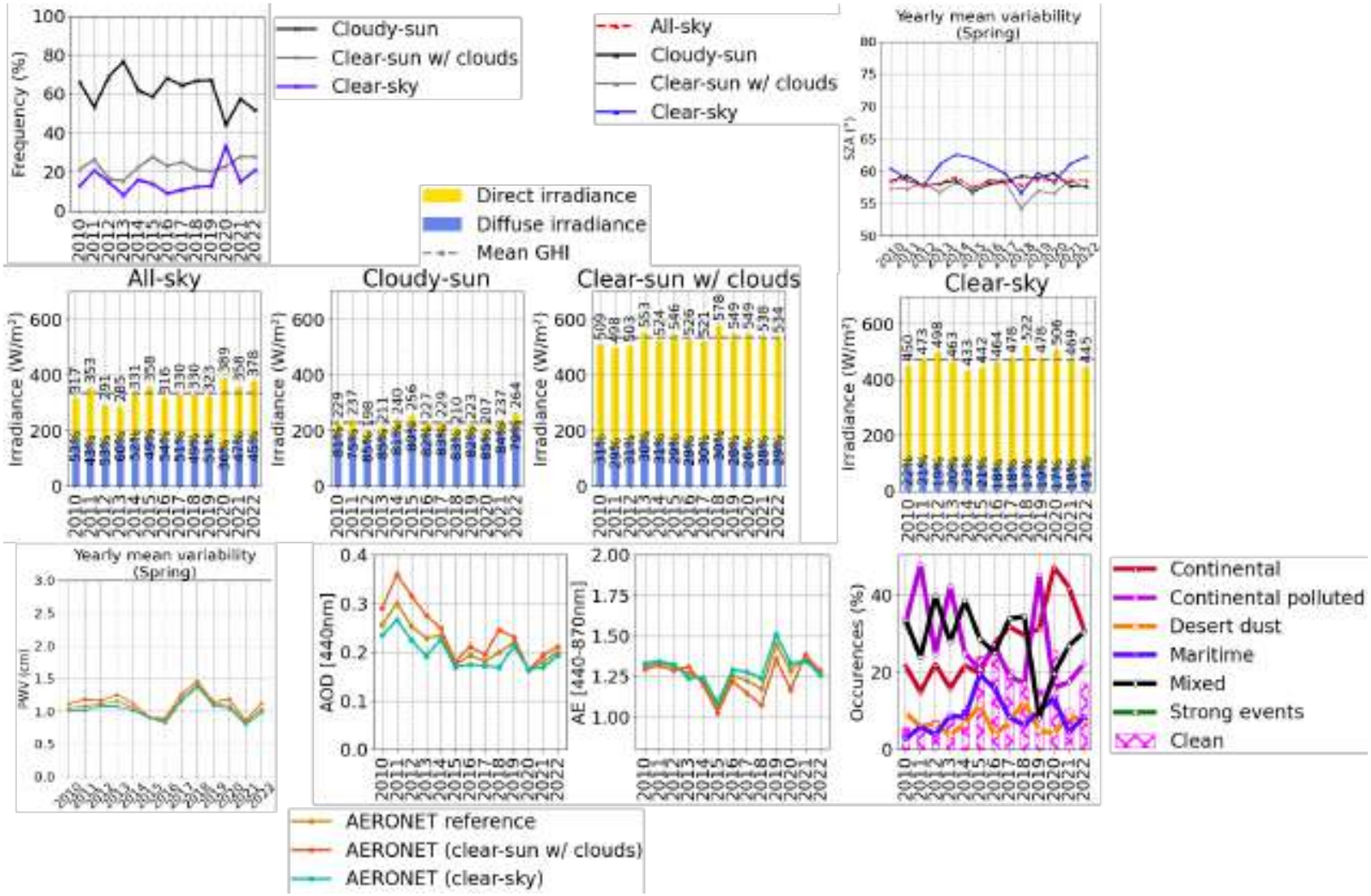

Yearly variability of all the parameters in Summer over 2010-2022

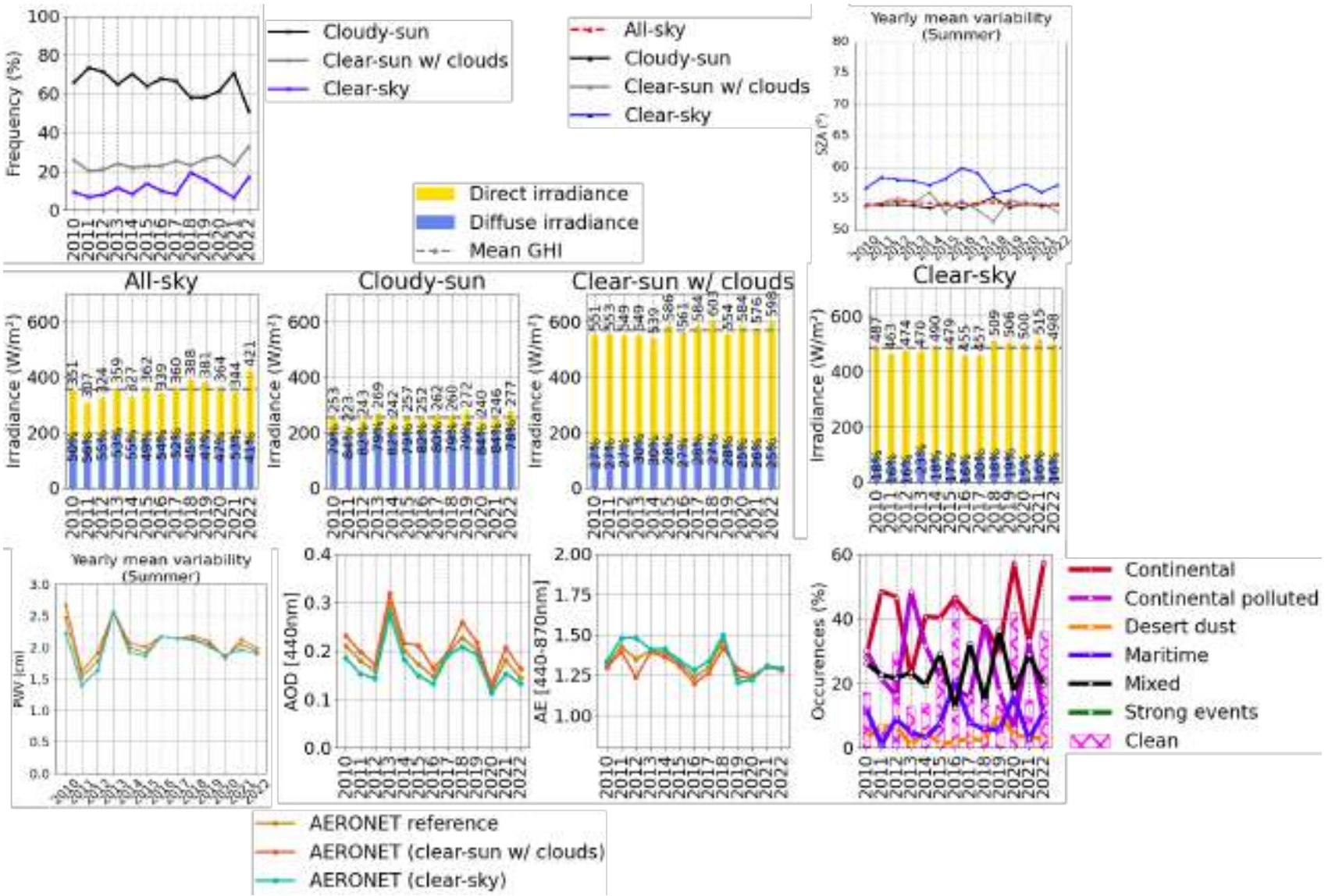

Decomposition of all-sky irradiances seasonal yearly variability in terms of clear-sky, clear-sun w/ clouds and cloudy-sun irradiances

$$F_{\text{all-sky},y} = \sum_k F_{k,y} \times f_{k,y}$$ **Changes in frequency**

$$\Rightarrow \Delta F_{\text{all-sky},y} = \sum_k \Delta F_{k,y} \times f_{k,y} + F_{k,y} \times \Delta f_{k,y}$$

Changes in irradiance

- $F_{\text{all-sky},y}$: Yearly mean seasonal all-sky irradiances (GHI, BHI, DHI)
- $F_{k,y}$: Yearly mean seasonal irradiances of the «k-th» sky condition (clear-sky, clear-sun w/ clouds, cloudy-sun)
- $f_{k,y}$: Yearly mean seasonal frequencies of the «k-th» sky condition
- $\Delta F_{\text{all-sky},y}$: Computed yearly seasonal deviations of all-sky irradiances to the 2010-2022 seasonal mean
- $\Delta F_{k,y}$ & $\Delta f_{k,y}$: Corresponding yearly seasonal deviations to the 2010-2022 seasonal mean under the «k-th» sky condition

Observed trends of the different parameters over 2010-2022

		Winter	Spring	Summer	Autumn
		Linear fit	Linear fit	Linear fit	Linear fit
GHI (W/m²)	Cloudy-sun	(-0.389 ± 0.670)x + (81.295 ± 4.570)	(0.267 ± 1.313)x + (224.584 ± 9.284)	(0.631 ± 1.161)x + (247.109 ± 8.206)	(1.272 ± 0.710)x + (137.472 ± 5.020)
	Clear-sun w/ clouds	(1.702 ± 2.137)x + (237.619 ± 14.569)	(3.336 ± 1.425)x + (512.849 ± 10.077)	**(3.732 ± 1.185)x + (545.917 ± 8.382)**	(2.024 ± 2.426)x + (377.076 ± 17.158)
	Clear-sky	(1.932 ± 2.668)x + (201.830 ± 18.192)	(1.345 ± 1.994)x + (462.720 ± 14.099)	**(3.082 ± 1.261)x + (466.418 ± 8.920)**	(2.402 ± 2.472)x + (337.034 ± 17.483)
	All-sky	(1.084 ± 1.205)x + (111.570 ± 8.218)	**(3.950 ± 1.901)x + (309.528 ± 13.439)**	**(4.210 ± 1.853)x + (327.877 ± 13.102)**	(2.911 ± 1.130)x + (201.085 ± 7.989)
BHI (W/m²)	Cloudy-sun	(-0.049 ± 0.148)x + (5.665 ± 1.008)	(-0.447 ± 0.649)x + (42.470 ± 4.589)	(0.090 ± 0.614)x + (46.554 ± 4.344)	(-1.366 ± 0.753)x + (23.629 ± 5.322)
	Clear-sun w/ clouds	**(2.093 ± 1.661)x + (149.162 ± 11.324)**	**(3.695 ± 1.073)x + (352.164 ± 7.585)**	**(3.837 ± 1.208)x + (387.422 ± 8.543)**	(1.481 ± 1.989)x + (253.139 ± 14.067)
	Clear-sky	(2.191 ± 2.431)x + (144.509 ± 16.579)	(2.267 ± 2.076)x + (363.120 ± 14.679)	**(3.080 ± 1.331)x + (379.456 ± 9.415)**	(1.942 ± 2.552)x + (264.544 ± 18.043)
	All-sky	**(1.367 ± 1.036)x + (35.978 ± 7.063)**	**(4.357 ± 2.304)x + (141.281 ± 16.292)**	**(4.656 ± 1.887)x + (145.439 ± 13.344)**	(0.985 ± 1.083)x + (89.344 ± 7.657)
DHI (W/m²)	Cloudy-sun	(-0.342 ± 0.538)x + (75.657 ± 3.667)	(0.717 ± 0.789)x + (182.134 ± 5.577)	**(0.536 ± 0.591)x + (200.620 ± 4.179)**	**(3.246 ± 1.396)x + (111.631 ± 9.874)**
	Clear-sun w/ clouds	(-0.391 ± 0.657)x + (88.457 ± 4.482)	(-0.359 ± 0.610)x + (160.685 ± 4.315)	(-0.106 ± 0.549)x + (158.495 ± 3.879)	(0.543 ± 0.589)x + (123.936 ± 4.162)
	Clear-sky	(-0.259 ± 0.353)x + (57.320 ± 2.406)	**(-0.922 ± 0.286)x + (99.601 ± 2.026)**	(0.002 ± 0.763)x + (86.962 ± 5.396)	(0.460 ± 0.535)x + (72.490 ± 3.780)
	All-sky	(-0.284 ± 0.448)x + (75.615 ± 3.055)	(-0.407 ± 0.772)x + (168.265 ± 5.457)	(-0.450 ± 0.463)x + (182.483 ± 3.272)	**(2.266 ± 1.049)x + (110.504 ± 7.420)**
AOD	Total	**(-0.004 ± 0.002)x + (0.144 ± 0.013)**	**(-0.008 ± 0.002)x + (0.260 ± 0.014)**	(-0.004 ± 0.003)x + (0.212 ± 0.023)	(-0.002 ± 0.002)x + (0.164 ± 0.016)
	Clear-sun w/ clouds	**(-0.005 ± 0.002)x + (0.154 ± 0.013)**	**(-0.011 ± 0.003)x + (0.308 ± 0.020)**	(-0.004 ± 0.003)x + (0.231 ± 0.024)	(-0.003 ± 0.003)x + (0.183 ± 0.018)
	Clear-sky	**(-0.004 ± 0.002)x + (0.137 ± 0.017)**	**(-0.006 ± 0.002)x + (0.231 ± 0.013)**	(-0.003 ± 0.003)x + (0.189 ± 0.022)	(-0.001 ± 0.002)x + (0.151 ± 0.016)
PWV	Total	(0.002 ± 0.008)x + (0.706 ± 0.055)	(-0.003 ± 0.012)x + (1.085 ± 0.083)	(-0.008 ± 0.021)x + (2.092 ± 0.149)	(-0.013 ± 0.021)x + (1.672 ± 0.149)
	Clear-sun w/ clouds	(-0.001 ± 0.008)x + (0.684 ± 0.053)	(-0.004 ± 0.013)x + (1.153 ± 0.090)	(-0.016 ± 0.021)x + (2.204 ± 0.149)	(-0.019 ± 0.018)x + (1.744 ± 0.130)
	Clear-sky	**(0.011 ± 0.010)x + (0.747 ± 0.066)**	(-0.002 ± 0.011)x + (1.041 ± 0.080)	(0.004 ± 0.022)x + (1.955 ± 0.156)	(-0.011 ± 0.025)x + (1.627 ± 0.175)
Proportions	Cloudy-sun	(-0.583 ± 0.775)x + (78.276 ± 5.284)	(-0.983 ± 0.598)x + (67.993 ± 4.228)	**(-0.918 ± 0.400)x + (70.452 ± 2.828)**	(-0.100 ± 0.452)x + (70.068 ± 3.193)
	Clear-sun w/ clouds	(0.516 ± 0.586)x + (15.797 ± 3.997)	(0.418 ± 0.258)x + (20.285 ± 1.823)	**(0.478 ± 0.205)x + (21.249 ± 1.451)**	(0.050 ± 0.234)x + (19.883 ± 1.654)
	Clear-sky	(0.066 ± 0.221)x + (5.934 ± 1.504)	(0.560 ± 0.485)x + (11.782 ± 3.429)	(0.441 ± 0.283)x + (8.306 ± 1.998)	(0.049 ± 0.301)x + (10.068 ± 2.125)
SZA	Cloudy-sun	(0.142 ± 0.076)x + (74.932 ± 0.515)	(0.018 ± 0.061)x + (58.270 ± 0.432)	(0.044 ± 0.033)x + (53.780 ± 0.232)	(0.015 ± 0.035)x + (68.263 ± 0.248)
	Clear-sun w/ clouds	(-0.022 ± 0.109)x + (74.667 ± 0.743)	(-0.026 ± 0.093)x + (57.509 ± 0.656)	(-0.094 ± 0.088)x + (54.508 ± 0.622)	(-0.030 ± 0.120)x + (66.358 ± 0.852)
	Clear-sky	(-0.056 ± 0.145)x + (76.340 ± 0.988)	(0.041 ± 0.142)x + (59.835 ± 1.002)	(-0.098 ± 0.089)x + (58.103 ± 0.629)	(-0.068 ± 0.144)x + (67.734 ± 1.016)
Occurences (Clear-sky)	Continental	(1.157 ± 1.949)x + (37.438 ± 13.287)	**(1.721 ± 0.528)x + (22.489 ± 3.734)**	(0.443 ± 0.997)x + (46.325 ± 7.047)	(-1.335 ± 1.222)x + (53.046 ± 8.643)
	Continental polluted	(-0.222 ± 0.933)x + (8.085 ± 5.826)	**(-0.886 ± 0.816)x + (29.521 ± 5.771)**	(-1.495 ± 0.911)x + (28.591 ± 6.440)	(0.250 ± 0.695)x + (10.041 ± 4.914)
	Maritime	(-0.020 ± 1.739)x + (36.375 ± 11.857)	(-0.051 ± 0.388)x + (8.465 ± 2.741)	(0.213 ± 0.407)x + (6.248 ± 2.879)	(1.348 ± 0.860)x + (10.697 ± 6.080)
	Desert dust	(0.190 ± 0.264)x + (2.400 ± 1.651)	(-0.006 ± 0.217)x + (4.942 ± 1.534)	(0.264 ± 0.275)x + (1.568 ± 1.943)	(-0.076 ± 0.407)x + (5.812 ± 2.880)
	Mixed	(-0.817 ± 0.894)x + (14.836 ± 6.094)	(-0.760 ± 0.744)x + (34.404 ± 5.263)	(0.575 ± 0.632)x + (17.269 ± 4.466)	(-0.188 ± 0.775)x + (20.404 ± 5.480)

Seasonal trends validated by a Mann-Kendall non-parametric test with a significance level of 5% are highlighted in bold text.

Decomposition of all-sky irradiances seasonal trends in terms of clear-sky, clear-sun w/ clouds and cloudy-sun irradiances

$$F_{all\text{-}sky} = \sum_k F_k \times f_k$$

$$\Rightarrow dF_{all\text{-}sky} = \sum_k \underbrace{dF_k \times f_k}_{\text{Trends in irradiance}} + \underbrace{F_k \times df_k}_{\text{Trends in frequency}}$$

- $F_{all\text{-}sky}$: Mean seasonal all-sky irradiances (GHI, BHI, DHI)
- F_k & f_k : Mean seasonal irradiances & frequencies of the «k-th» sky condition (clear-sky, clear-sun w/ clouds, cloudy-sun)
- $dF_{all\text{-}sky}$: Computed trends in all-sky irradiances over 2010-2022
- dF_k & df_k : Observed trends in irradiances and frequency over 2010-2022 under the «k-th» sky condition

Classification of the observed aerosol optical properties*

Objective

- Characterize the aerosol content and its variability
- Create locally defined aerosol properties models for radiative transfer simulations using AERONET inversions

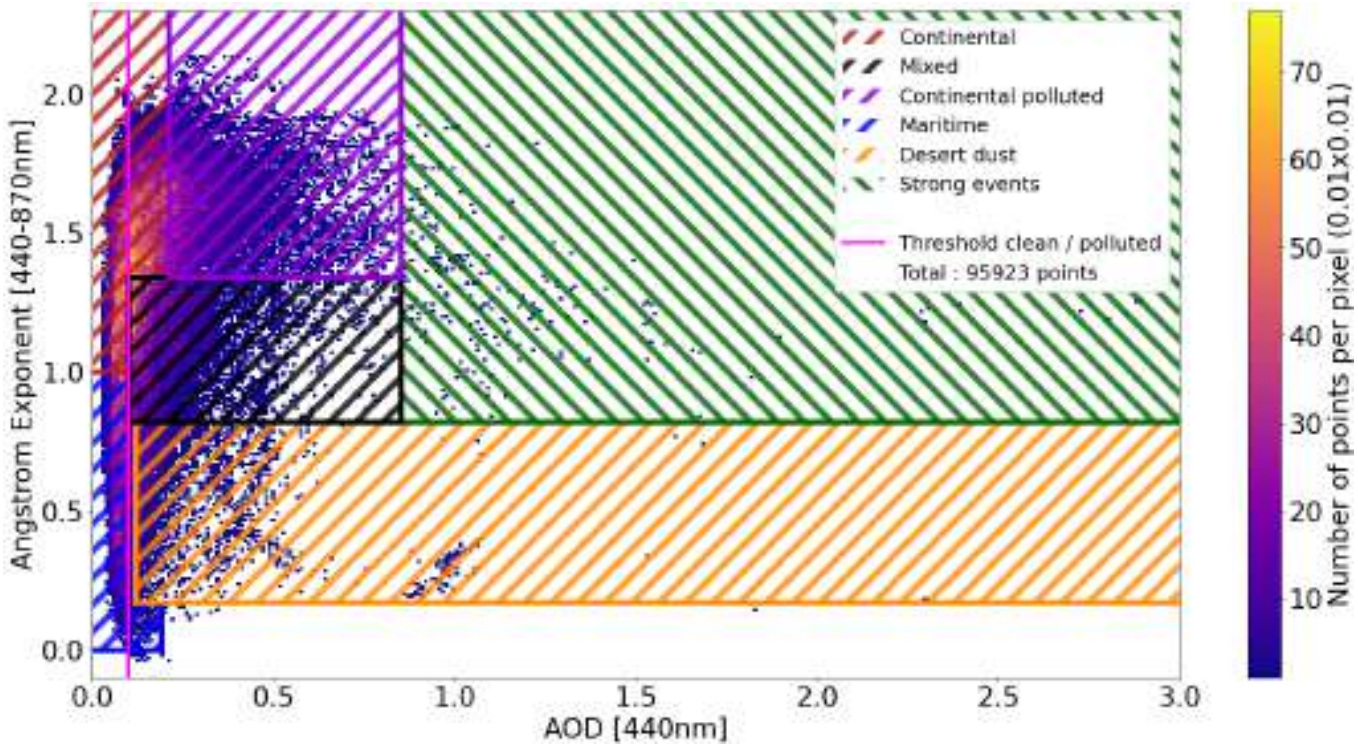

*Inspired by the work of Toledano et al. (2007)

SOLARTDECO radiative transfer simulations

Objective

- Simulate the surface solar global irradiance and its components
- Evaluate their sensitivity to the aerosol content in clear-sky conditions

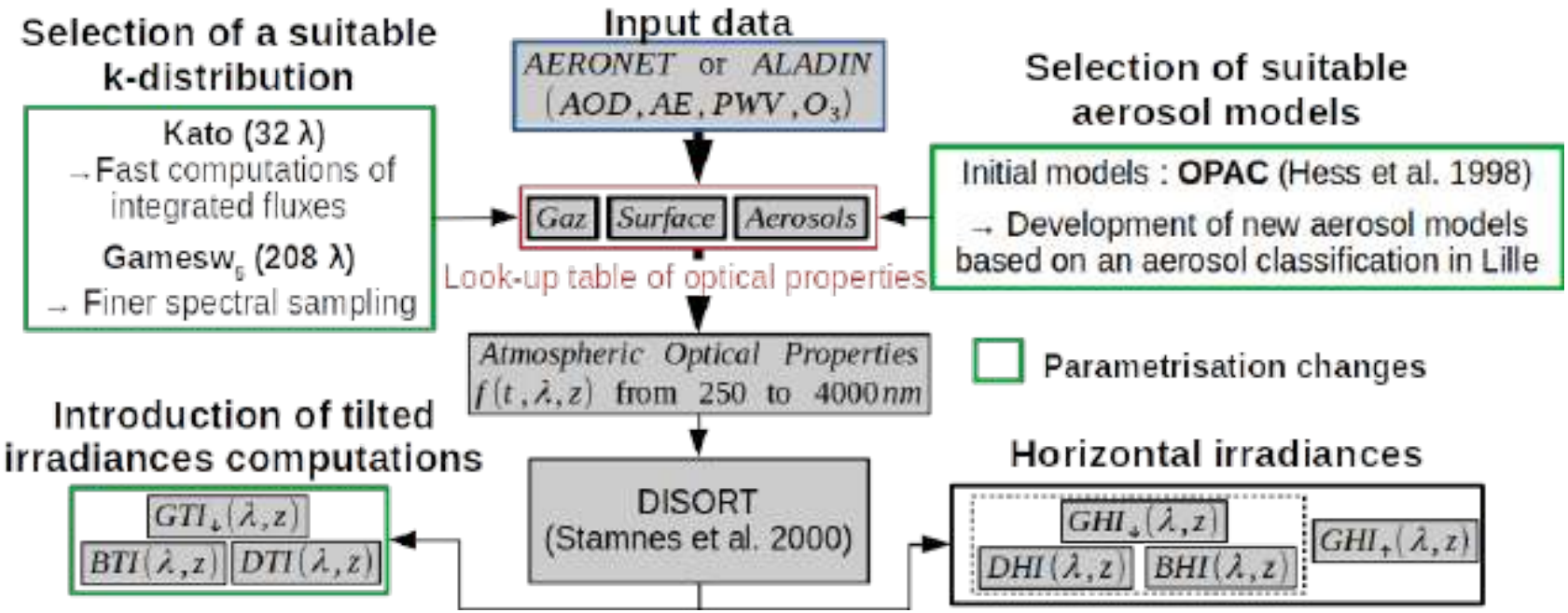

Validation of SOLARTDECO clear-sky simulations over 2010-2022

Method: Comparisons against ground 1-min irradiance measurements in clear-sky conditions over 2010-2022 for DNI values greater than 120 W/m² and for times between [sunrise + 30 minutes; sunset - 30 minutes].

		GHI	BHI	DHI
SOLARTDECO	Bias (W/M²) [%]	(0.76) [0.18]	(-1.09) [0.13]	(1.85) [2.40]
	RMSD (W/m²) [%]	(9.06) [2.66]	(7.27) [3.14]	(7.21) [8.06]
McClear	Bias (W/M²) [%]	(0.26) [0.22]	(-7.78) [-1.99]	(8.03) [11.75]
	RMSD (W/m²) [%]	(12.96) [3.96]	(28.56) [11.26]	(20.50) [23.76]
Number of comparisons		44235		

Decomposition of the clear-sky irradiances seasonal yearly variability in terms of aerosol optical properties

$$F_{clear,\ y} = \sum_i F_{clear,\ i,\ y} \times f_{clear,\ i,\ y}$$

$$\Rightarrow \Delta F_{clear,\ y} = \sum_i \Delta F_{clear,\ i,\ y} \times f_{clear,\ i,\ y} + F_{clear,\ i,\ y} \times \Delta f_{clear,\ i,\ y}$$

$$\Delta F_{clear,\ i,\ y} = \sum_x \left[\frac{\partial F_{clear}}{\partial x}\right]_{i,\ y} \times \Delta x_{clear,\ i,\ y}$$

$$\left[\frac{\partial F_{clear}}{\partial x}\right]_{i,\ y} \approx \left[\frac{F_{clear}(x+\delta x,\ \alpha_1,\ \ldots,\ \alpha_n) - F_{clear}(x,\ \alpha_1,\ \ldots,\ \alpha_n)}{\delta x}\right]_{i,\ y}$$

- $F_{clear,y}$: Yearly mean seasonal clear-sky irradiances (GHI, BHI, DHI)
- $F_{clear,i,y}$: Yearly mean clear-sky seasonal irradiances for the «i-th» aerosol class (Continental, Continental Polluted, Mixed, Maritime, Desert dust)
- $f_{clear,i,y}$: Yearly mean seasonal frequencies of the «i-th» aerosol class under clear-sky conditions
- $dF_{clear,y}$ & $dF_{clear,i,y}$ & $df_{clear,i,y}$: Corresponding yearly seasonal deviations to the 2010-2022 seasonal means
- $\left[\frac{\partial F_{clear}}{\partial x}\right]_{i,\ y}$: Seasonal sensitivities to a change of +1% in the yearly mean of parameter «x» for the «i-th» class in clear-sky conditions
- α_j : Other parameters (AOD, SSA, SZA, PWV), beside «x», needed for computations of the sensitivities

Decomposition of the clear-sky irradiances seasonal trends in terms of aerosol optical properties

$$F_{clear} = \sum_i F_{clear,\ i} \times f_{clear,\ i}$$

$$\Rightarrow dF_{clear} = \sum_i dF_{clear,\ i} \times f_{clear,\ i} + F_{clear,\ i} \times df_{clear,\ i}$$

$$dF_{clear,\ i} = \sum_x \left[\frac{\partial F_{clear}}{\partial x}\right]_i \times dx_{clear,\ i}$$

$$\left[\frac{\partial F_{clear}}{\partial x}\right]_i \approx \left[\frac{F_{clear}(x+\delta x,\ \alpha_1,\ \ldots,\ \alpha_n) - F_{clear}(x,\ \alpha_1,\ \ldots,\ \alpha_n)}{\delta x}\right]_{i,}$$

- F_{clear} : Mean seasonal clear-sky irradiances (GHI, BHI, DHI)
- $F_{clear,i}$: Mean clear-sky seasonal irradiances for the «i-th» aerosol class (Continental, Continental Polluted, Mixed, Maritime, Desert dust)
- $f_{clear,i}$: Mean seasonal frequencies of the «i-th» aerosol class under clear-sky conditions
- dF_{clear} & $dF_{clear,i}$ & $df_{clear,i}$: Corresponding seasonal trends to the 2010-2022 seasonal means
- $\left[\frac{\partial F_{clear}}{\partial x}\right]_i$: Seasonal sensitivities to a change of +1% in the mean of parameter «x» for the «i-th» class in clear-sky conditions
- α_j : Other parameters (AOD, SSA, SZA, PWV), beside «x», needed for computations of the sensitivities

Validation of ALADIN-climat HINDCAST simulations

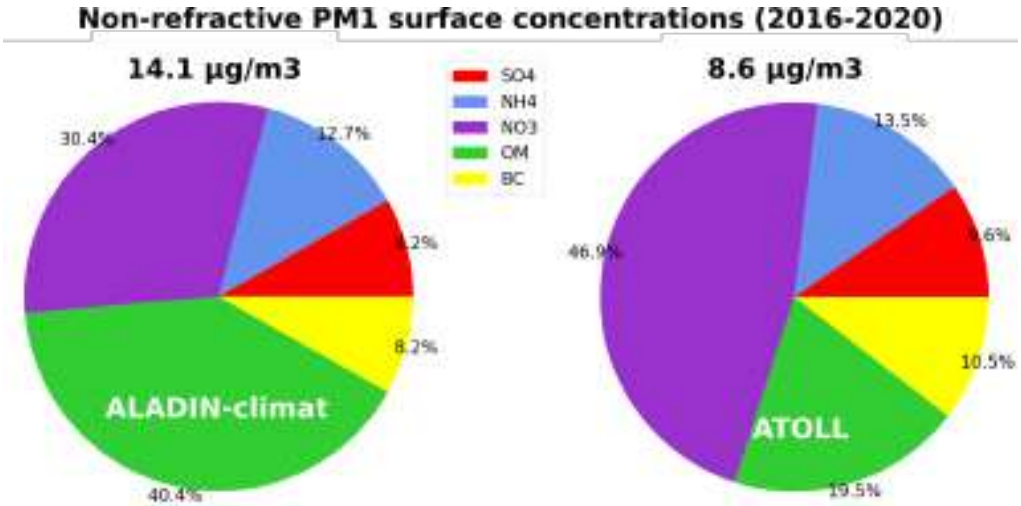

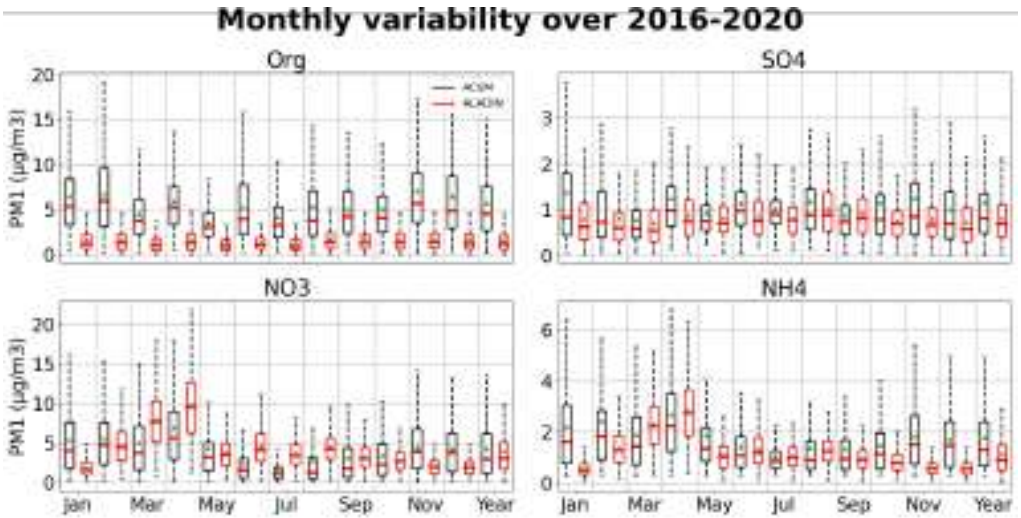

Future evolution of the surface temperature

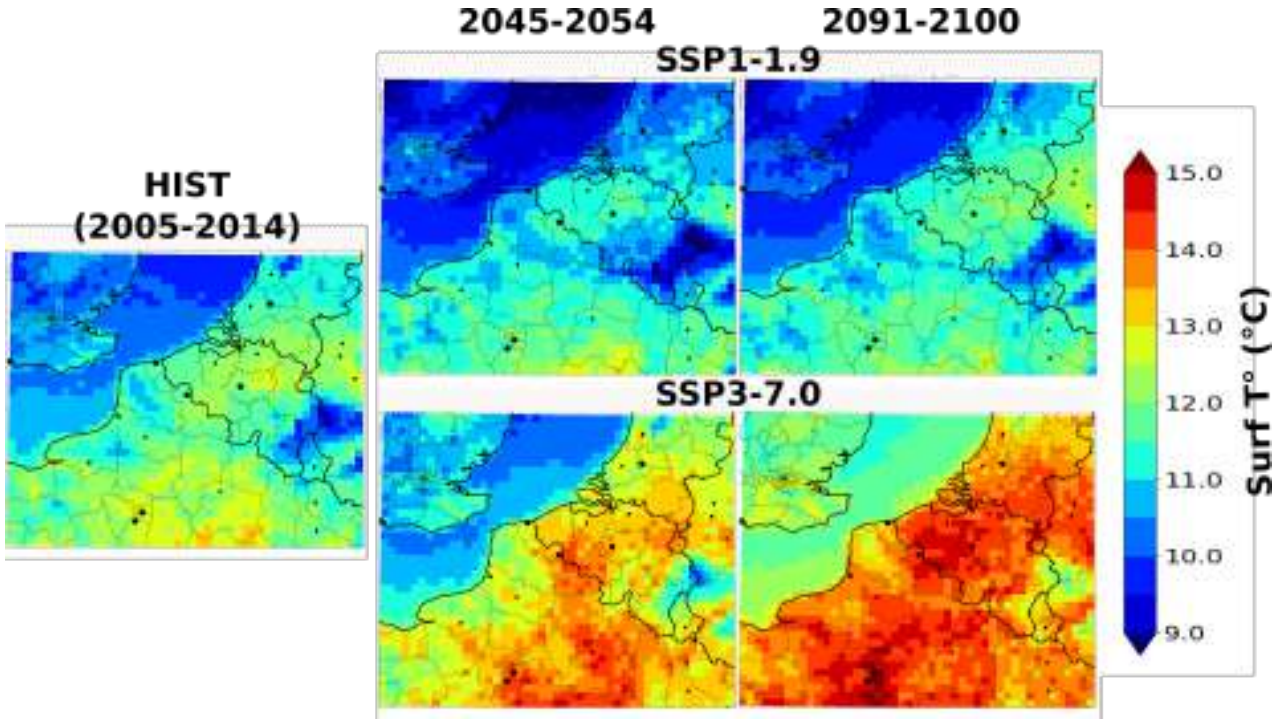

- SSP1-1.9 :
  - **Stable surface temperature ∼ 11-13℃ over land compared to HIST**
  - **Slight decrease ∼ -0.5℃ over/near the sea**
- SSP3-7.0 :
  - **Important increase by end of century ∼ +1-2℃ over both land and sea**
  - **Corresponding increase in water vapor from ∼ 1 cm to ∼ 1.2 cm**

Future evolution of the precipitable water vapor content

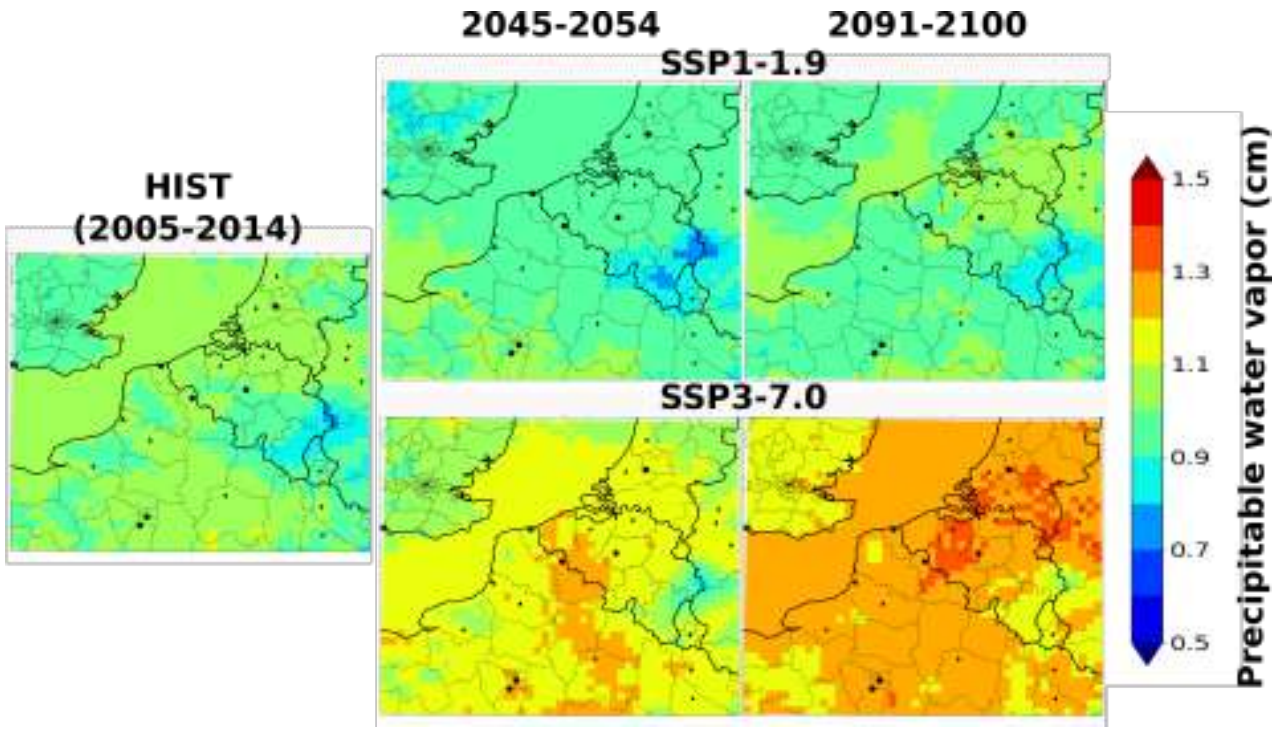

References

Batlles, F. J. et al. (2000). "Comparison of Cloudless Sky Parameterizations of Solar Irradiance at Various Spanish Midlatitude Locations". In: *TAC*. DOI: 10.1007/s007040070034.

Dubovik, Oleg and Michael D. King (2000). "A flexible inversion algorithm for retrieval of aerosol optical properties from Sun and sky radiance measurements". In: *JGR*. DOI: https://doi.org/10.1029/2000JD900282.

García, R. D. et al. (2014). "Solar radiation measurements compared to simulations at the BSRN Izaña station. Mineral dust radiative forcing and efficiency study". In: *JGR*. DOI: https://doi.org/10.1002/2013JD020301.

Gidden, M. J. et al. (2019). "Global emissions pathways under different socioeconomic scenarios for use in CMIP6: a dataset of harmonized emissions trajectories through the end of the century". In: *GMD*. DOI: 10.5194/gmd-12-1443-2019.

Long, Charles N. and Thomas P. Ackerman (2000). "Identification of clear skies from broadband pyranometer measurements and calculation of downwelling shortwave cloud effects". In: *JGR*. DOI: https://doi.org/10.1029/2000JD900077.

Nabat, Pierre et al. (2020). "Modulation of radiative aerosols effects by atmospheric circulation over the Euro-Mediterranean region". In: *ACP*. DOI: 10.5194/acp-20-8315-2020.

Toledano, C. et al. (2007). "Aerosol optical depth and Angstrom exponent climatology at El Arenosillo AERONET site (Huelva, Spain)". In: *QJRMS*. DOI: https://doi.org/10.1002/qj.54.